Author Statement

Manuscript title: An Anchoring Array Assembly Method for Enhancing the Electrical Conductivity of Composites of Polypropylene and Hybrid Fillers

All persons who have made substantial contributions to the work were reported in the manuscript：

Jiashu Zhu and Xiaolong Gao do the experiment of Composites of Polypropylene and Hybrid Fillers; Chaoying Wan and Tony McNally designed the material system and revised the paper; Hong Xu and Ying Liu designed the mold; Jian Zhuang and Jingyao Sun designed the hot embossing machine; Yao Huang and Daming Wu analyzed the data.

Yao Huang

Department of Electrical and Mechanical Engineering

Beijing University of Chemical Technology

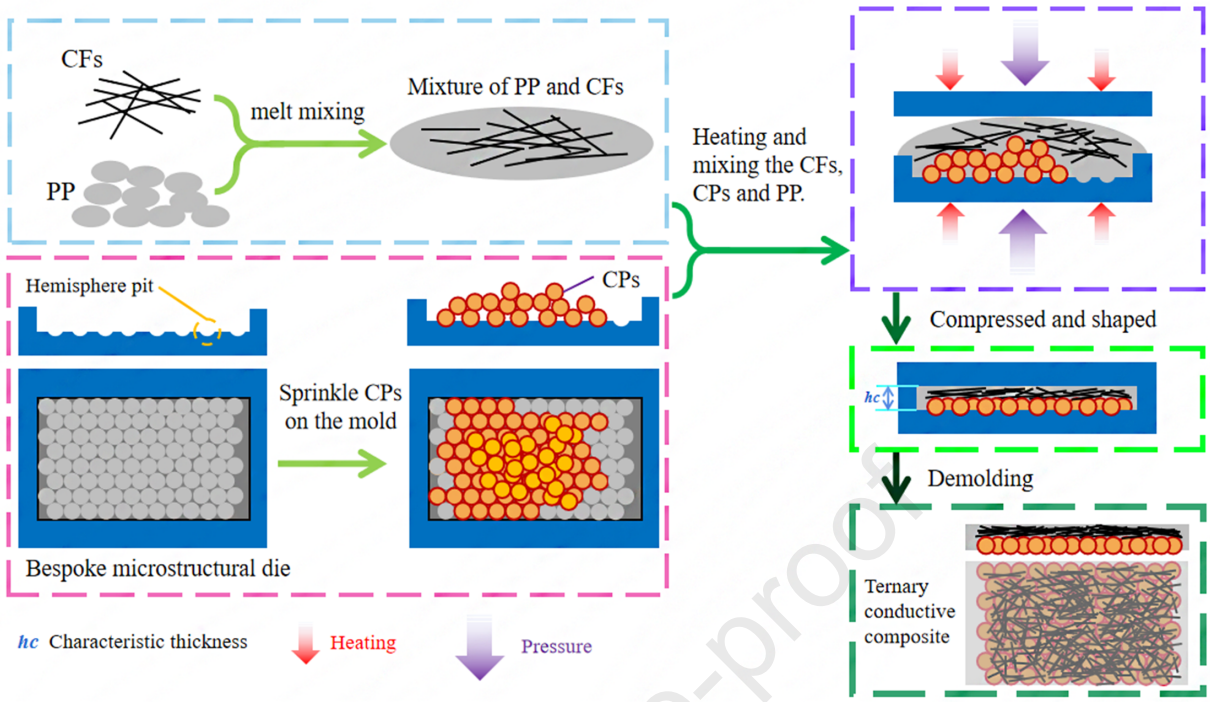

An Anchoring Array Assembly Method for Enhancing the Electrical Conductivity of Composites of Polypropylene and Hybrid Fillers

Jiashu Zhu[a], Chaoying Wan[b], Hong Xu[a], Ying Liu[a], Jian Zhuang[a], Jingyao Sun[a], Xiaolong Gao[a], Tony McNally[b*], Yao Huang[a]*, Daming Wu[a,c]*

a. College of Mechanical and Electrical Engineering, Beijing University of Chemical Technology, Beijing 100029, China.

b. International Institute for Nanocomposites Manufacturing (IINM), WMG, University of Warwick, Coventry, UK.

c. State Key Laboratory of Organic-Inorganic Composites, Beijing University of Chemical Technology, Beijing, 100029, China.

* Correspondence: hy06@163.com (Y.H.); t.mcnally@warwick.ac.uk (T.McN); wudaming@vip.163.com (D.W.);

ABSTRACT: Constructing an interconnected filler-filler network in a polymer matrix is essential for enhancing the electrical conductivity of polymer composites. This work describes an Anchoring Array Assembly method for distribution of copper particles (CP) and carbon fibers (CF) in a polypropylene (PP) matrix. Constrained by a predesigned array anchoring template, the CP distribution achieved a high packing density in the PP matrix during compression molding which is key for filling the gaps between CFs, as well as for forming an interconnected hybrid filler network. Using the fixed array anchoring design, the dispersion and flow behavior of the conductive fillers and the polymer matrix are critical. When the inclination angle between the groove of the anchor mold and the horizontal plane was greater than 11.5 °, the migration of CP in the molten PP when in the anchor mold during the hot embossing process is restricted. The most conductive composites were obtained when the CPs were densely arranged in a triangular format. The conductive filler network was determined by the preset dense triangular "island-bridge" structure of the customized microarray mold. The conductivity of the composites prepared by the anchoring array assembly method reached 137.70 S/m, some 52 times higher than that prepared by traditional hot embossing methods with the same filler loading.

Keywords: Composites; Polymer processing; Electrical conductivity; Anchoring Array Assembly Method

1. Introduction

Polymer-based functional composites are obtained from the mixing of one or more organic or inorganic fillers with a polymer matrix via physical or chemical methods, with the aim of achieving a combination of synergetic properties, such as electrical and thermal conductivity and, or mechanical reinforcement [1-6]. Electrically conducting polymer-based composites can be prepared using conductive polymers or by mixing of conductive fillers with insulating polymers, the latter has the advantage of large-scale manufacture and a wide range of different blend components. However, the enhancement in the electrical conductivity of filled polymer composites is often at the expense of mechanical properties and processability. This is due to the dual challenges of effective dispersion of conductive fillers and poor interfacial interactions between the filler and polymer matrix. To date, different approaches have been attempted to address these technical challenges, such as surface modification of conducting fillers to improve dispersion and interfacial interactions with polymers, filler orientation or combinations of hybrid fillers added to polymers to facilitate the formation of conducting filler networks.

Xu et al. [7] reported a new method for constructing a co-continuous morphology of a continuous polymer phase and a continuous conductive filler network using 3D printing methods. The fabricated carbon nanotube (CNT)/thermoplastic polyurethane composites showed simultaneously enhanced electrical conductivity and mechanical properties. This processing method was easy to design and accurately shaped the conductive network, but the composites was relatively thick, and difficult to form in to a sheet for further shaping. Cao et al. [8] investigated the dispersion of carbon black (CB) aggregates in a polystyrene melt by measuring both the resistance and dynamic storage modulus as a function of annealing time. The aggregation of CB in the polystyrene melt was closely related to the terminal relaxation of the polystyrene, and the interfacial tension between polystyrene and CB determined the formation of CB aggregates.

Deng et al. [9] studied the manufacture of conductive polymer fibers by controlling the morphology of the conductive network. A two-component ribbon/fiber composite was prepared using multi-walled carbon nanotubes (MWCNTs) and a low

melting point polymer (LMP) filled with CB. The bi-component tape/fiber contains two layers of conductive polymer composite (CPC) with a higher melting temperature than the LMP. The unfilled polymer core is manufactured by melt extrusion. The shape control of the conductive network formed by the nanowire array was achieved by physical stretching and annealing. The final composites were obtained by secondary melt co-extrusion. This method results in the fillers between polymers to form a ribbon/fibrous network with good conductivity, which can be used for sensing, smart textiles, as electrodes for flexible solar cells and in electromagnetic interference (EMI) shielding. However, the filler packing density is low and therefore filler-filler network formation limited.

Zhang et al. [10] aggregated conductive fillers by adding secondary polymers with a stronger binding force to conductive fillers on the basis of self-assembly, to achieve enhanced electrical properties of the composite. It was found that the secondary polymer has the effect of attracting clusters of the conductive filler that had been initially agglomerated in the polymer matrix. Cai et al. [11] combined shearing and electrostatic treatment on a flowing polymer melt which aligned the conductive fillers in the polymer melt over a large area. The authors found that a variety of conductive fillers (e.g. silver-plated microspheres, carbon nanotubes (CNTs) and graphene) had limited effect when oriented on application of an electric field, magnetic field, or shear induction alone. Christoph et al. [12] studied the relationship between fiber length and content and the mechanical and electrical properties of injection molded short carbon fiber (CF) reinforced polypropylene (PP) composites. The authors found that the electrical conductivity and mechanical properties of the composites (except the elongation at break) were linearly related to the average fiber length.

Wu et al. [13] prepared conductive composites of PP and short CF using a spatial confining forced network assembly (SCFNA) method utilizing a conical twin-screw mixer and space-limited compression. The conductivity of the composites was 4 orders of magnitude higher than those prepared by extrusion and compression molding. In addition, the SCFNA process is able to process thin films with dense conductive filler networks not achieved by conventional processing methods. To

further increase the electrical conductivity of the composites the, design and formation of interconnecting filler-filler conducting networks are critical.

When shortened CF is added to a polymer, it is difficult to control the filler network due to the mobility of the fiber in the resin [14]. In this work, a method of assembling and anchoring a filler particle array is proposed, and a compression mold with a microarray structure designed to shape the fiber network. Copper particles (CPs) are introduced to the composites as anchor points for the CF network. With the array microstructure template of the mold, the CPs are anchored at designated positions to form an anchor point array, and the CFs used to bridge the anchor points, so that a conductive network is formed during a compression molding process. The conductive fibers or fillers are thus confined in-plane by the anchoring structure of the composites, and a second filler type (CPs) will fill the space of the first filler network and form a regular and dense conductive filler/fiber network structure.

In this work, a new Anchoring Array Assembly Method is described by incorporating both conductive CFs and CPs into PP, and the method used to shape and control an electrically conducting CF-CP network within in the PP matrix.

2. Experimental

2.1 Materials

CPs (YUPLENE BX3900) were supplied by the Institute of Metal Research, Chinese Academy of Sciences (CAS), having a particle size 80 mesh (diameter 0.2 mm) and density 8.96×10^{-3} g/mm^3. PP was purchased from Korean SK global chemical production and had an MFI of 0.25 to 38 g/10min and a density of 0.891 to 0.910 g/cm^3) Short cut carbon fibers (SCF) of 4 mm in length, 7 μm in diameter and an electrical conductivity of 2.6×10^4 S/m were supplied by Toray, Japan

2.2 Preparation of PP/CP/CF ternary composites

A conical twin-rotor mixer (HAAKE) was used for mixing the PP/CP/CF composites. The imprint equipment utilized was bespoke, designed and assembled in-house.

The anchoring array assembly (using array microstructure assisted molding) method was compared with traditional hot embossing (plate structure). Seven samples with different filler concentrations were prepared using each processing method.

(1) Preparation using the traditional hot embossing method as a control. PP was dry blended with 2 vol.% CP firstly, then mixed with 2 to 18 vol.% CF using a HAAKE internal mixer at 50 rpm, 170 °C for 10 minutes. The composite samples obtained were then compression molded at 10 MPa ,170 °C for 30 minutes. The thickness of the samples produced was 1mm.

(2) Preparation using anchoring hot embossing method. PP was firstly dry blended with 2 vol.% CP, then mixed with 2 to 18 vol.% CF using a HAAKE internal mixer at 50 rpm, 170 °C for 10 minutes. In order to perform compression molding at 10 MPa, the CPs were placed in a pre-designed triangular array anchor mold and uniformly dispersed on the surface of the micro-structured mold by means of ultrasonic treatment. Then, the mixed PP-CF composite sheet and the dispersed CP on the mold are subjected to hot embossing for 30 minutes. Composites with CF volume content of 2 % to 18 % were prepared with thicknesses between 0.2 mm to 1 mm.

2.3 Characterization and testing

Characterization of the composite laminates was performed by placing a sample of each composite in a JTVMS-1510T image measuring instrument (manufactured by Dongguan Jiateng Instrument Company) to observe the macro-morphology of the contact surface of the material on the micro-array structure, and the arrangement of the CPs in the conductive network. Then scanning electron microscopy (Phenom Desktop SEM, magnification: 100-410 times, voltage: 15 KV, no sputter coating of the sample before imaging) was used to observe the microscopic morphology through the cross section of the sample. Finally, the electrical properties of the ternary conductive composites were measured using a four-point probe method (4200-SCS) at 20 ℃[11].

In order to test the mechanical properties of the material, a tensile fracture test was performed on the samples at a strain rate of 10 mm/min. using an INSTRON5567 machine. The spline was rectangular with a width of 25 mm and, the total length of the test sample was 60 mm (25 mm clamped up and down).

3. Results and Discussion

3.1 Formation of conducting networks via the Anchoring Assembly Method

Firstly, a bespoke microstructural die was designed in order to arrange the fillers into a triangular conductive network in the polymer matrix. As illustrated in Figure 1, the PP/conductive filler composite is firstly prepared by mechanical blending. In the process of compression molding, the composite is firstly compressed and shaped under pressure, and then compressed further until a 'characteristic thickness' (i.e. 3~5 times larger than the filler diameter) is reached. As such the filler spacing within the assembled network is reduced to the desired value, while the density of the network is greatly enhanced. Determined by the CP diameter and the designed filler network shape, the size (microstructure) and array form of the mold are designed to achieve the anchor assembly of CPs, such that the CFs can only be distributed in the thin layer region outside the gap because of its larger size, finally giving a controlled assembly of a conductive filler-filler network. By adjusting the thickness of the sample and further reducing the thickness, CPs and CFs can be closer to each other or in contact, thus forming a conductive network between conductive fillers.

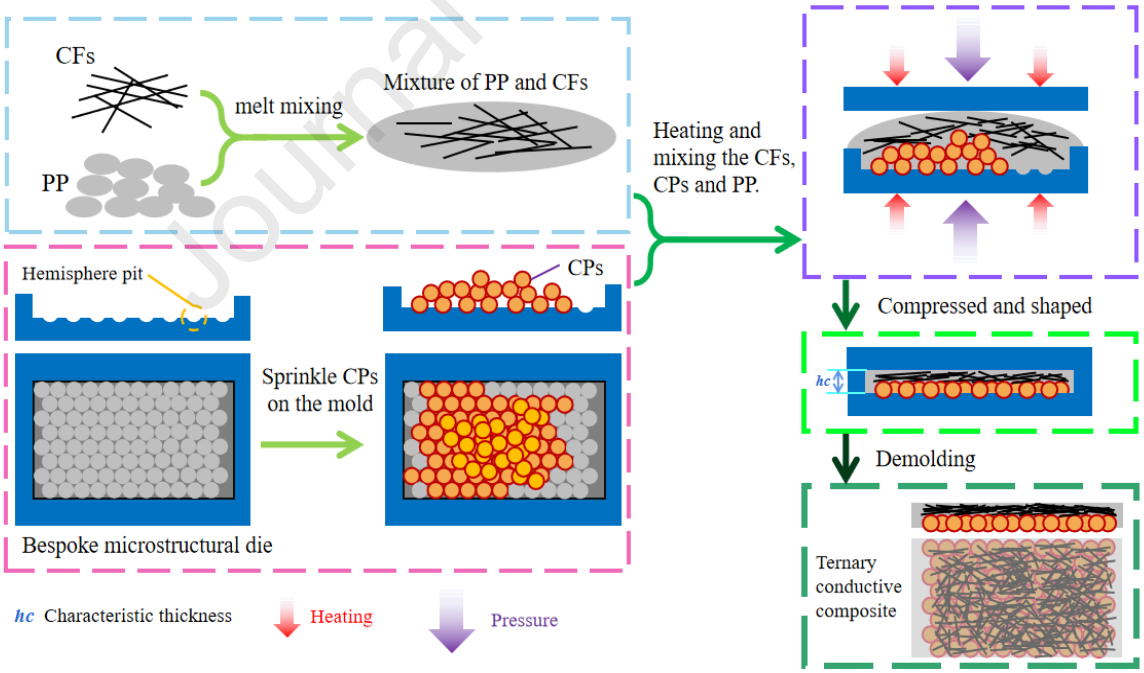

Figure 1. Schematic illustration of the anchorage and space-bound forced assembly for the preparation of ternary composites.

The combination of CPs and CFs forms an 'island-bridge structure' conductive network, that is, a "node island" of CPs connected by a 'bridge' of CFs, thus forming

a conducting ‘fishing-net like’ circuit where the number of CPs ’node islands’ will determine the conductivity of the whole conducting network.

The shape, size and material properties of the conductive fillers and their interactions with the polymer matrix will govern the conductivity of the composites. The electrical properties of the composites containing spherical conductive fillers were therefore simulated and analyzed using circuit simulation software [15,16].

For composites, electrical conductivity is related to the filler type, the average spacing between fillers and the overlapping of fillers. Correspondingly, from previous research, the simulation and prediction of the electrical properties of composites has been described by three mechanisms, (1) Percolation theory [17], (2) Quantum tunneling theory [18-21] and (3) simple overlapping of filler particles within the composite to form a conductive network [22,23]. Of these, percolation theory is used to deal with systems with strong disorder and random structure [17]. Quantum tunneling theory requires the average spacing between fillers to be on the nanometer scale [18-21]. Due to the limitation and arrangement of the CPs of the array structure, it can be considered that the conductivity of these composites is derived from overlapping and touching of the filler particles to form a conductive network within the PP matrix.

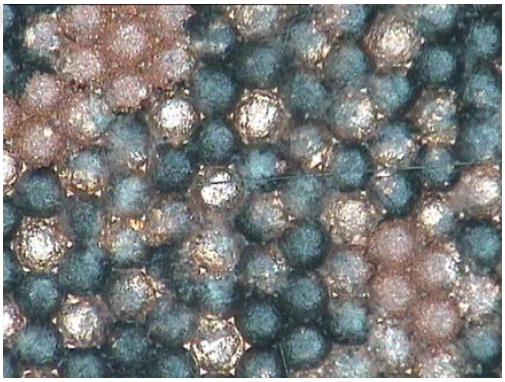

Figure 2. Photograph of the surface of a composite showing the microstructure obtained (CF 4 vol.%, CP 2 vol.%).

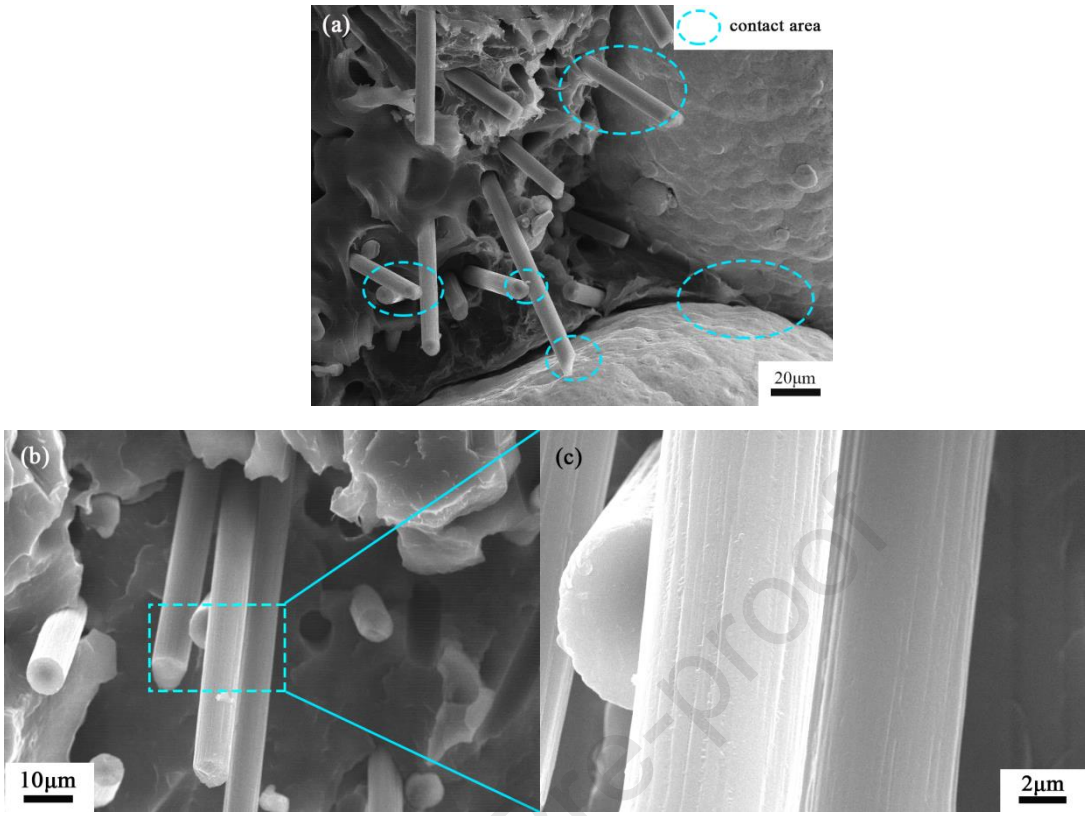

Figure 3. SEM images showing contact points between fillers within the composites, (a) contact between CPs, (b) between CF and CP and (c) contacts between CFs.

As shown in Figure 2 and Figure 3, it is found that the conductive filler particles are in contact (whether between CFs, CPs or between CF and CP). Therefore, the conductivity model can be described by the Greenwood–Tripp (GT) model. This model can estimate the contact effect between most rough surfaces, as it is often used to simulate and calculate the contact between materials with certain elastic deformation.

According to the published literature [24-27], the main conductive ability of composites comes from the contact between fibers. This requires estimation and calculation of contact resistance accounting for fiber arrangement.

Zhiliang Wu [24] et al. optimized the relationship between the contact resistance between different particles and, the relationship between the particles in contact was proposed by Holm [25] as follows:

$$R_c = \frac{\rho_1 + \rho_2}{4\sqrt{A_c / \pi}} \tag{1}$$

where, R_c is the particle contact resistance, ρ_1 and ρ_2 is the resistivity of the contact particles, and A_c is the micro-contact area (may be circular, elliptical or multi-point contact). A_c has the following relationship [24-26]:

$$A_c = \pi R_e \delta \tag{2}$$

where, R_e is the equivalent radius, which is:

$$R_e = R_1 \sqrt{\frac{R_2}{R_1 + R_2}} \tag{3}$$

where, R_1 and R_2 are the radii of the two kinds of filler particles (the granular filler is the radius of the sphere, and the cylindrical filler is the cross-sectional radius). δ is the equivalent elastic compression distance of the particle contact point. This distance is related to the equivalent elastic modulus and equivalent compressive load.

The equivalent elastic compression distance can be determined from:

$$F_c = \frac{4}{\left(3E^* \times R_e^{1/2} \times \delta^{3/2}\right)} \tag{4}$$

where, F_c is the compressive load, E^* is the equivalent elastic modulus, and E^* can be calculated from Hertz contact theory [27,28] using the relevant formula [25,26]:

$$E^* = \frac{1}{\left(\left(1 - \frac{\upsilon_{CP}^2}{E_{CP}}\right) + \left(1 - \frac{\upsilon_{CF}^2}{E_{CF}}\right)\right)} \tag{5}$$

where, E_{CP}, E_{CF}, υ_{CP}, and υ_{CF} are the Young's modulus and Poisson's ratio of the CPs and CFs, respectively. The processing method employed requires compression of the composites but, there will also be a certain amount of ‘extrusion’ or lateral flow between the fillers which will also result in contact between the fillers.

When the CFs are in contact, the following situations will occur: the fibers are overlapped perpendicularly, the fibers are non-vertically overlapped and the fibers are end faced overlapped [27]. In reality, most of the situations that appear are vertical and non-vertical overlapping and, end-face overlapping is rare [27-29]. Due to the limitation of the CP spheres arranged in an array in the composites, the fibers will form three network arrangements: linear, a cross array and a dense triangular array. Of these, the linear and cross-array contact is mainly vertical overlap, and the contact

resistance can be calculated in the same manner using equations (1) through (5). In the dense triangular array, since the acute angle between the two fibers is likely to be 60 °, the micro-area in contact can be considered as a circle (semi-spherical) into an elliptical (semi-elliptical) area [24]. This can be determined from the geometric relationship that the micro-contact area in the dense triangular array is $3^{0.5}$ (i.e. about 1.73 times) that of the conventional area.

The mechanical and electrical properties of the two fillers are shown in the Table 1:

Table 1. Mechanical and electrical properties of the CP and CF fillers

Filler type	Filler modulus of elasticity (MPa)	Filled Poisson's Ratio (m)	Filler conductivity (S/m)	Filler resistivity (Ω·m)	Filler particle morphology	Filler morphological parameters
CP	1.19×10^{5}	0.307	5.71×10^{7}	1.75×10^{-8}	Sphere	radius:0.05mm
CF	2.5×10^{5}	0.326	2.6×10^{4}	3.85×10^{-5}	Cylinder	Cross section radius:7μm Long：4mm

The resistance of the different types of contact points and related coefficients were calculated and are shown in the Table 2:

Table 2. Contact resistance related data for the different types of contact points

Contact type	E^{*} (MPa)	R_e (m)	F_c (N^{-1})	δ (m)	A_c (m^2)	R_c (Ω)	Contact resistance (CP-CP as R_{CP})
CF-CP	0.5	1.84×10^{-5}	94.02	3.52×10^{-4}	2.03×10^{-8}	0.12	$2941\times R_{CP}$
CP-CP	0.5	3.50×10^{-4}	94.02	1.32×10^{-4}	1.45×10^{-7}	4.08×10^{-5}	R_{CP}
CF-CF(90°)	0.5	4.95×10^{-6}	94.02	5.46×10^{-4}	8.49×10^{-9}	0.37	$9069\times R_{CP}$
CF-CF(60°)	0.5	4.95×10^{-6}	94.02	5.46×10^{-4}	1.47×10^{-8}	0.28	$6863\times R_{CP}$

From previous experiments [16, 30, 31], three basic network forms can be considered in the simulation:

1. CPs are arranged linearly

The internal structure, partial area structure and equivalent circuit of the expected composite material are shown in Figure 4.

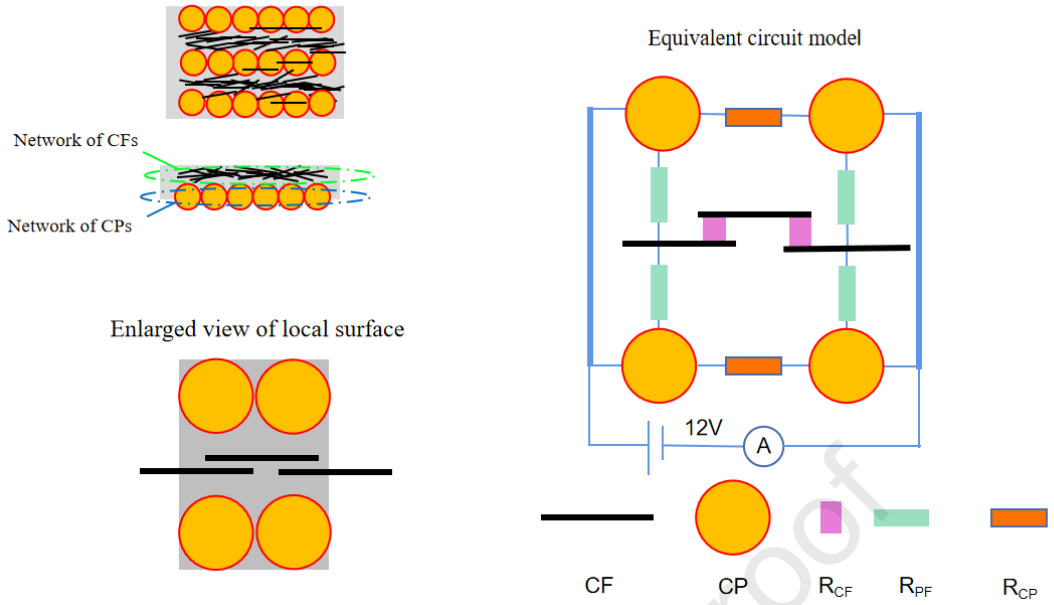

Figure 4. CP structure diagram and its equivalent circuit arranged when the CP are arranged linearly.

2. CPs are arranged according to a crossed network

The internal structure, partial area structure and equivalent circuit of the expected material are shown in the Figure 5:

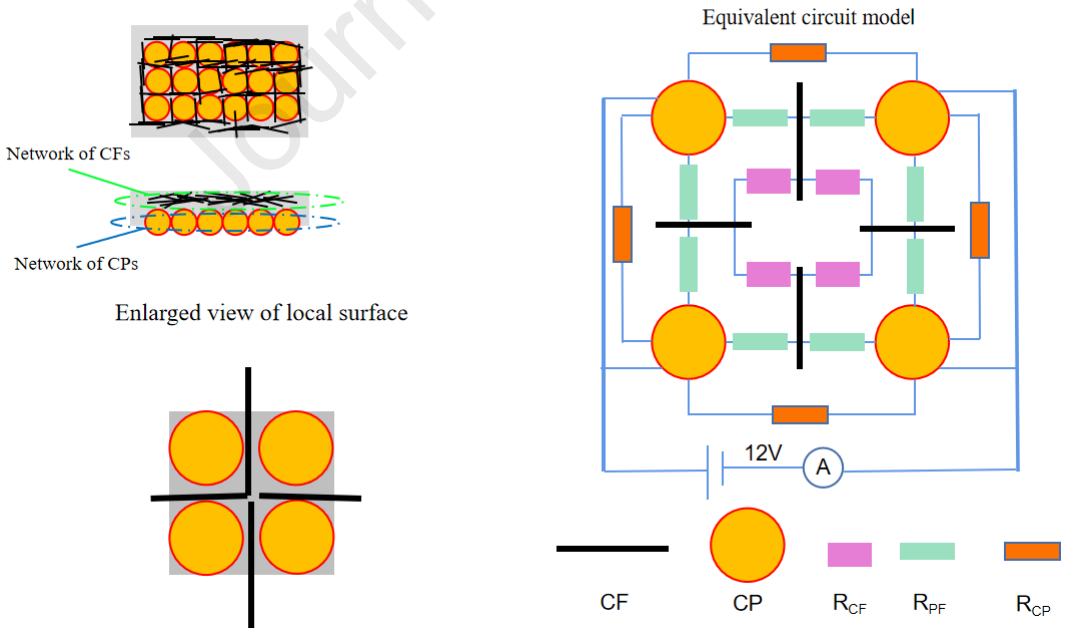

Figure 5. CP according to the cross-arrangement structure diagram and its equivalent circuit.

3. CPs are arranged in a dense triangular network

The internal structure of the material, the structure of some areas and the

equivalent circuit are shown in Figure 6:

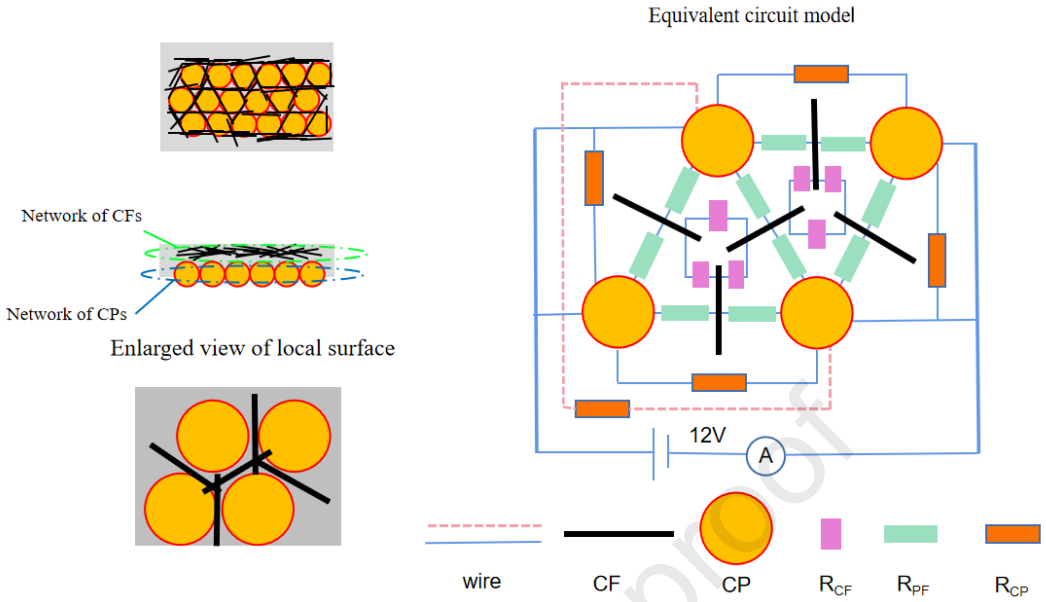

Figure 6. CP structure diagram and its equivalent circuit arranged for a dense triangular network.

In accordance with the preset resistance and the proportional relationship between the three resistances, simulation software [15] was used to predict the electrical properties of the three filler network types, see Table 3.

Table 3. Simulation results for the three types of filler networks in the PP matrix.

Network shape	Analog applied voltage (V)	Analog indication of ammeter (mA)	Conversion network equivalent resistance (Ω)
Linear	12	4.741	$2.53\times10^{3}\times R_{CP}$
Cruciform	12	5.709	$2.10\times10^{3}\times R_{CP}$
Dense triangle	12	7.279	$1.65\times10^{3}\times R_{CP}$

It can be seen from Table 3 that the equivalent resistance of the dense triangular network is the lowest ($1.65\times10^{3}\ R_{CP}$), which is the most conducive to improving the electrical conductivity of the composites.

3.2 Processing of the composites in the die: Mechanical theory

The CPs should be arranged in a preset position such that they do not move under the applied force of the mobile melt and the hot stamping machine. The force analysis of the CPs is carried out from the perspective of a polymer fluid mechanics

problem and the shape of the ball pit should be quantitatively designed. It is only in this way can the CPs be arranged according to the set requirements.

Therefore, it is necessary to clarify the flow mechanism between the two types of conductive fillers within the polymer matrix, as well as the geometric and dynamic conditions during the formation of the anchoring arrays. Taking the angle of the bevel as θ, which is used to restrict the movement of the CP, then the force and torque diagram for CPs on the die is given by Figure 7.

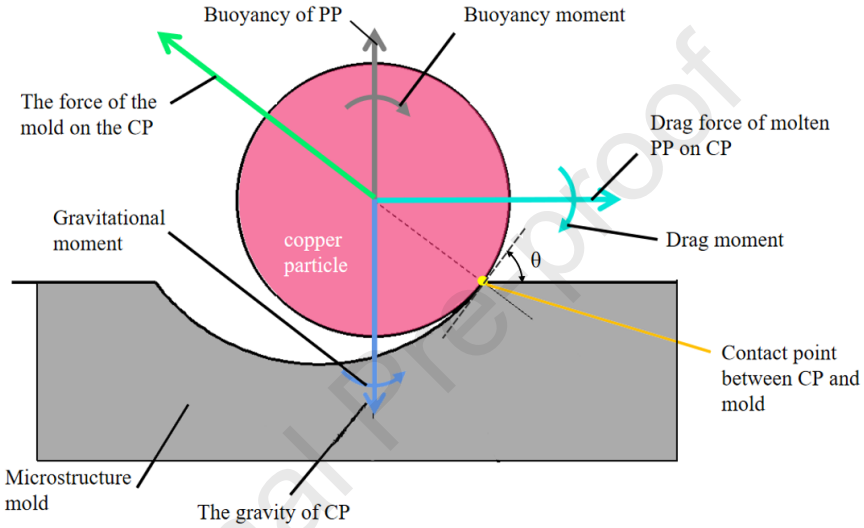

Figure 7. Force and moment diagram of a CP on the die surface.

From Figure 7, each CP is subjected to four forces as it flows through the PP, i.e. gravity, buoyancy of molten PP to the CP, the drag of the PP melt (fluid) on the CP and the force of the die on the CP. If the material was in equilibrium in this state, the force balance and the moment balance are considered as the two conditions. The condition for the force balance is expressed in equation 6:

$$\vec{F}_{mold}+\vec{F}_{gravity}+\vec{F}_{buoyancy}+\vec{F}_{drag}=0 \tag{6}$$

Here, the drag force of the PP melt (fluid) on a CP during the hot embossing process and when the flat plate pressing velocity was set as 1 mm/s, the molten PP diffused evenly in the plane perpendicular to the direction of pressing. The flow rate of PP in plane was V_1 = 0.212 mm/s. The maximum speed between the two plates was V_2 = 0.424 mm/s and the shear rate is expressed as in equation 7:

$$\dot{\gamma} = V_2 / （0.5d）= 0.848 s^{-1} \quad (7)$$

where, d is the distance between the two flat plates, the area under shear is A and the shear stress is given by [32-36]：

$$\tau = \frac{F}{A}, \quad \eta = \frac{\tau}{\dot{\gamma}} \quad (8)$$

According to [37, 38], the shear viscosity is: $\eta = 5600 Pa \cdot S$ and the shear stress is

$$\tau = \dot{\gamma} \cdot \eta = 4749 Pa \quad (9)$$

In equations 8 and 9, the shear area A was 1.41×10^{-7} m^2 and the drag force of the PP fluid on the CP was $F_{drag} = 6.71\times10^{-4}$ N, and the gravity of the CP was $F_{gravity} = 3.68\times10^{-3}$ N.

PP buoyancy to CP was $F_{buoyancy} = 3.79\times10^{-4}$ N. The calculated force terms can be therefore summarized as follows:

$$F_{buoyancy} = \mathrm{g} \cdot \rho_{PP} \cdot V_{Copper} = 3.79\times10^{-4} N \quad \text{Direction upward} \quad (10)$$

$$F_{gravity} = \mathrm{g} \cdot \rho_{C} \cdot V_{Copper} = 3.68\times10^{-3} N \quad \text{Direction downward} \quad (11)$$

$$F_{drag} = \tau_{PP} \cdot A = \eta_{PP} \dot{\gamma}_{PP} A = 6.71\times10^{-4} N \quad \text{Horizontal to right} \quad (12)$$

$$\vec{F}_{mold} = -(\vec{F}_{drag} + \vec{F}_{buoyancy} + \vec{F}_{gravity}) \quad (13)$$

$$F_{mold} = 3.37\times10^{-3} N \quad (14)$$

In equations 10 through 14, ρ_c is the density of CP, g was the acceleration due to gravity, V_{copper} was the volume of a single CP, ρ_{PP} was the density of PP and A is the acting surface of the shear force.

For the torque balance, the CP was subjected to 3 torques, with the counterclockwise being positive. θ is the inclined angle of the die or the tangent angle of the circular groove and the formulas for the respective torques are:

$$M_{all} = M_{gravity} + M_{buoyancy} + M_{drag} \quad (15)$$

$$M_{gravity} = G \times R_C \times \sin\theta \quad (16)$$

$$M_{buoyancy} = -1 \times F_{buoyancy} \times R_c \times \sin\theta \quad (17)$$

$$M_{drag} = -1 \times F_{drag} \times R_c \times \cos\theta \tag{18}$$

From the equations 15 through 18, when $M_{all} = 0$, $\theta = 11.49\,° \approx 11.5\,°$.

The radius of the ball pit was 0.15 mm (marked as "R"), the depth of the ball pit was 0.06 mm (marked as "h"), i.e. R/h = 2.5, which satisfies the restriction for the movement of the CPs. Theoretically, the die can be designed to restrict the flow of CPs between flat sheet materials where the CPs should be "anchored" to the microstructure mold and not move in the mold plane with the flow of molten PP. Based on the above calculations, the overall size of a single incomplete hemispherical pit/hole in the mold can be designed.

The holes are arranged in a tight triangular shape, which ensures that all the holes are tangential to each other from the upper surface, for the formation of a packing network. As shown in Figure 8, the triangular arrangement of the microstructure array ensures that the CPs are arranged in a pre-determined triangular network on one side.

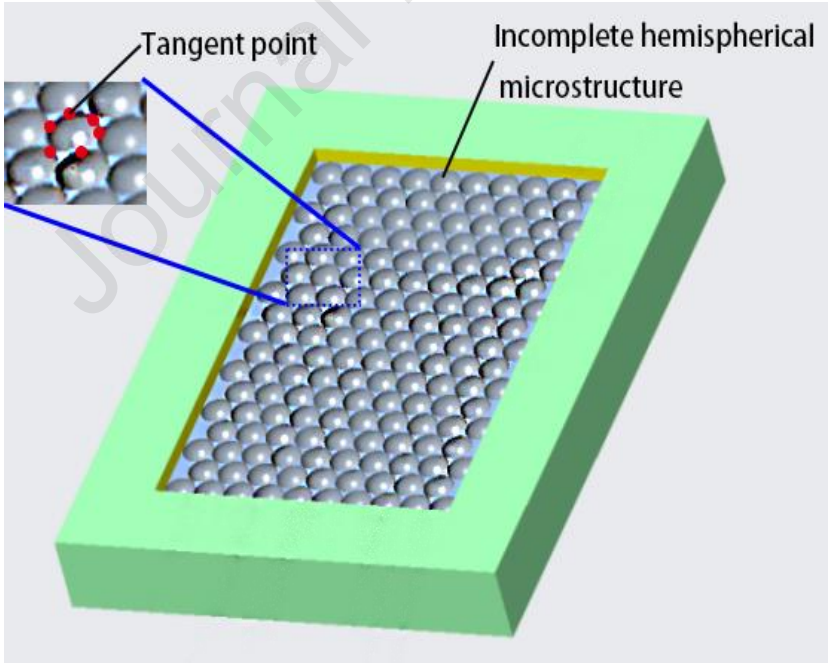

Figure 8. Schematic diagram of microarray structure.

While verifying the effectiveness of the anchoring array assembly method, the conductivity of the composites can be improved synergistically by forced compression of the mold to reduce the thickness of the sample, so as to construct a

more compacted filler-filler network in the PP matrix and in doing so achieve higher conductivity, as is shown schematically in Figure 9. As the thickness of the composites continues to decrease by forced compression of the mold, the CPs are compressed into the microstructure of the mold to form the triangular network, and the spacing between CFs and between CF and CP continues to decrease. When the number of overlapping points between larger-sized filler particles increases, the conductive paths formed throughout the composite increases, thereby reducing the overall resistance of the composites [24-29]. Therefore, it is relevant to reduce the thickness of the sample by forced compression of the mold on the basis of the assembly of the anchor array to increase the electrical conductivity of the composites.

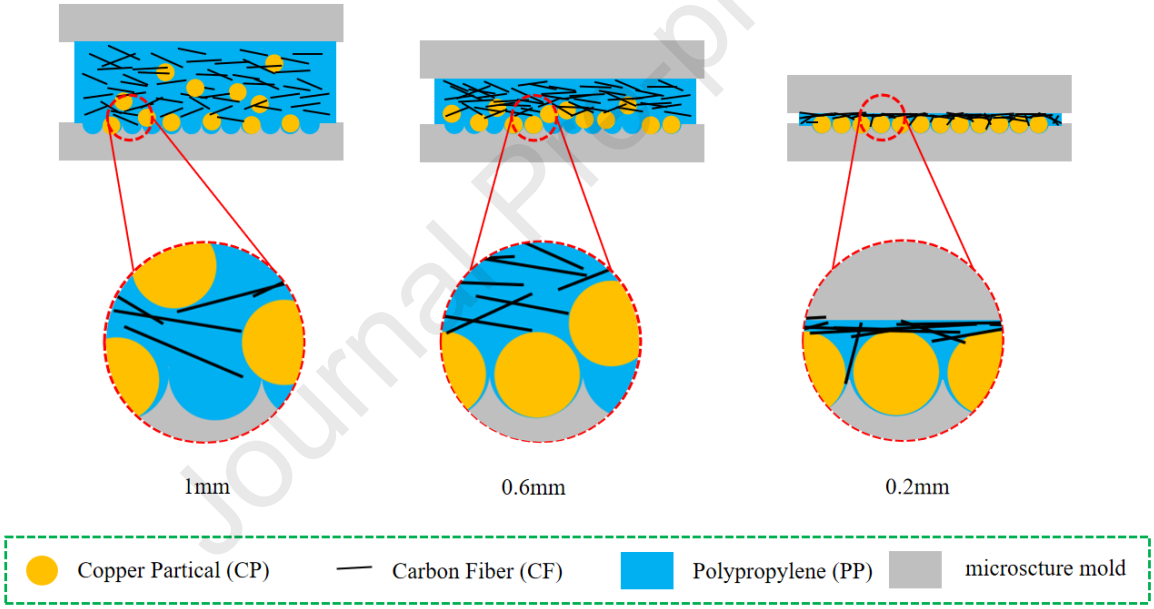

Figure 9. Cross-sectional schematic diagrams of conductive composites of different thicknesses.

In this paper, the volume ratio of fillers, the thickness of the sample and the processing method were used as independent variables. The dispersion of the fillers in the polymer matrix and the conductivity of composites was then evaluated by varying the volume ratios of the fillers with and without using the microarray die.

Table 4. Electrical performance test data for the Composites with varying filler ratio and loading

CF content (vol.%)	CP (vol.%)	Use of anchoring arrays to assist molding	Thickness (mm)	Resistance (Ω)	Electrical resistivity (Ω·m)	Electrical conductivity (S/m)
2	2	No	1	9616	53.42	0.019
3	2	No	1	6042	33.57	0.030
4	2	No	1	2500	13.89	0.073
5	2	No	1	1307	7.26	0.14
6	2	No	1	800	4.44	0.23
12	2	No	1	106	0.59	1.69
18	2	No	1	69	0.38	2.63
2	2	Yes	1	2681	14.89	0.068
3	2	Yes	1	2325	12.79	0.078
4	2	Yes	1	333	1.83	0.55
5	2	Yes	1	296	1.63	0.61
6	2	Yes	1	250	1.38	0.73
12	2	Yes	1	66	0.36	2.75
18	2	Yes	1	31	0.17	5.87
6	2	Yes	0.6	198	0.65	1.53
12	2	Yes	0.6	45	0.149	6.73
18	2	Yes	0.6	16	0.053	18.90
6	2	Yes	0.4	52.3	0.115	8.69
12	2	Yes	0.4	17.5	0.039	25.97
18	2	Yes	0.4	10.3	0.0227	44.10

6	2	Yes	0.2	21.2	0.023	42.90
12	2	Yes	0.2	10.6	0.0117	85.76
18	2	Yes	0.2	6.6	0.0073	137.70

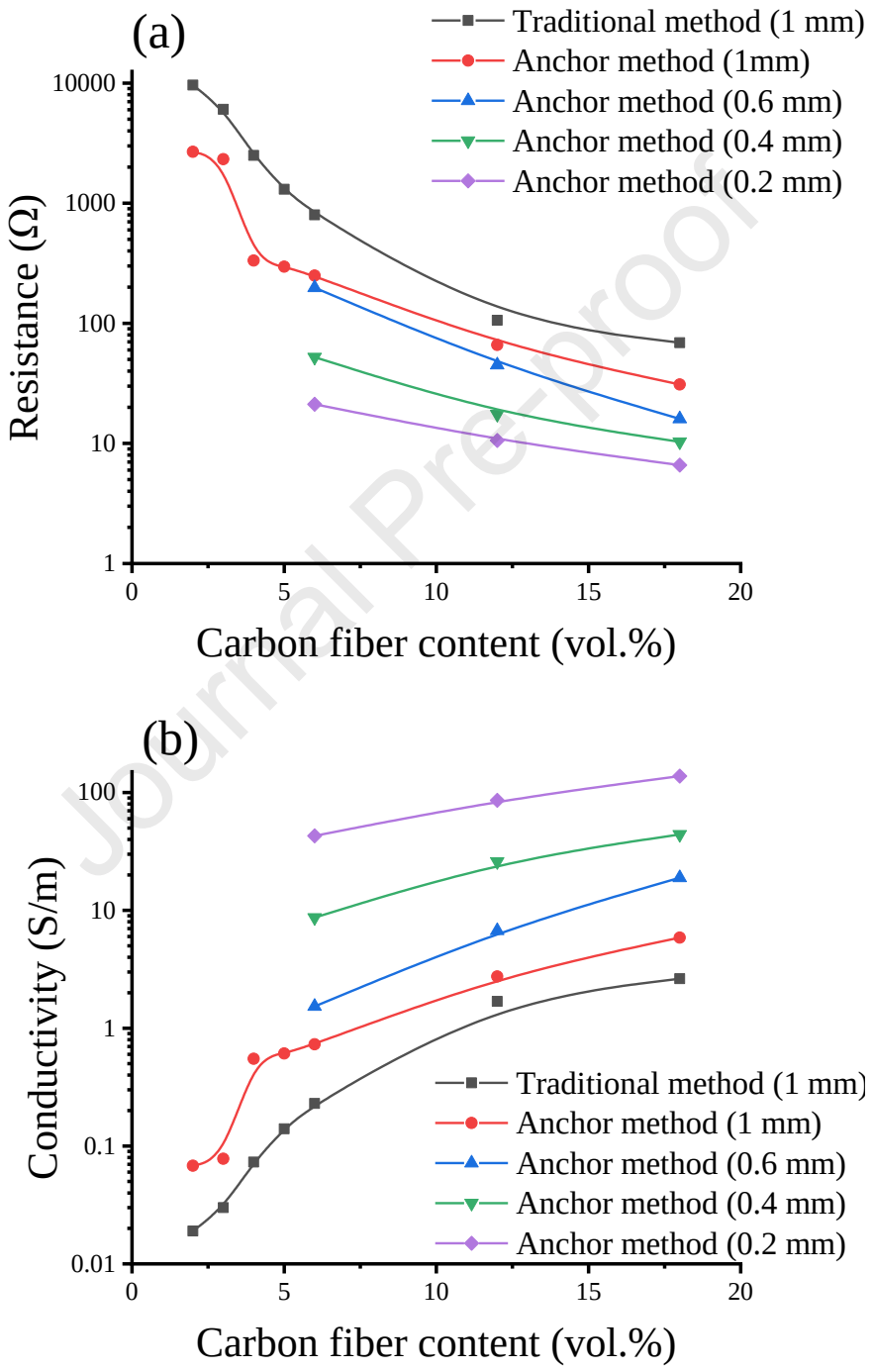

Figure 10. Effect of CF content and composite thickness on electrical properties (a) electrical resistance and (b) electrical conductivity.

It can be seen from Table 4 and Figure 10 that when the filler concentration is constant, the conductivity of the sample prepared by the anchoring array assembly method is higher than that of the traditional hot embossing method, up to 52 times (i.e. for a CF content 18 vol.% and CP content 2 vol.%). It can be seen from Figure 10 (b) that when the content of CF is greater than 3 vol.%, the increase in electrical conductivity (thickness of 1 mm) of the composite prepared by the anchoring array assembly method is larger than that of the traditional method. The response in Figure 10 (b) is that the CF concentration and conductivity curve of the anchoring array assembly method will show a more obvious uplift at 3 vol.%, while the curve growth of the traditional method is relatively smooth, and there is almost no obvious increasing trend. In contrast, the conductivity of samples prepared by traditional methods has almost a linear relationship with CF content. When the CF content is increased from 2 vol.% to 4 vol.%, the conductivity of the sample prepared by the traditional method increased by 3.8 times. The sample prepared by the anchoring array assembly method increased by 8.1 times. The electrical conductivity of the composite material continues to increase with decreasing composite thickness and increasing filler (CF) content (as shown in Figure 10 and Figure 2). When the content of CF reaches 18 vol.%, the content of CP is 2 vol.%, and the thickness of the composites is 0.2 mm, conductivity reaches the highest value of all samples, 137.70 S/m.

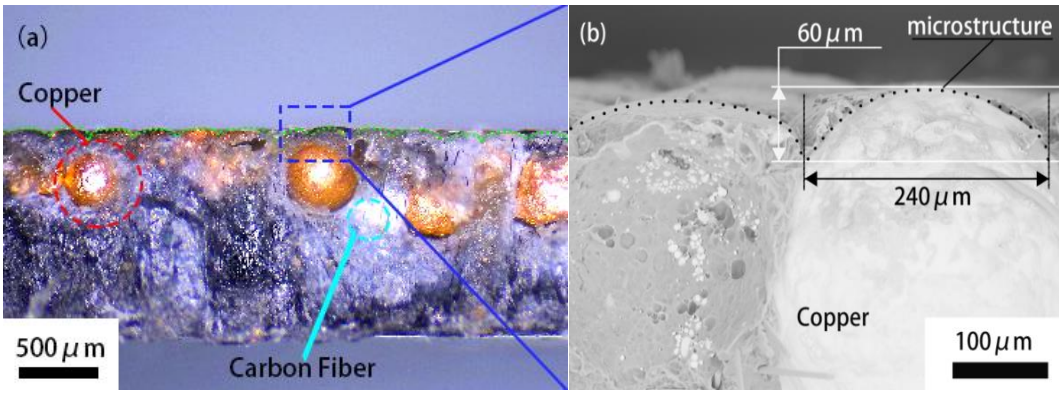

Figure 11. Cross-section of composite samples, a) an optical photograph and b) a SEM image of the microstructure of a molded composite.

Figure 11 shows that when using the micro-structured die, the CPs are arranged closely on one side of the material, where the CPs and CFs form a ‘tree-like’ conductive network in the PP matrix. The CPs are arranged in dense and regular triangles by anchoring arrays and the CFs overlap each other in the composites to form a dense "island-bridge" conductive network structure. This "island-bridge" conductive network places the conductive fillers (CPs and CFs) in close contact in the polymer matrix. As a result, the electrical resistance of the composites is reduced. The morphology of the composites is shown in Figure 11 (a) and (b).

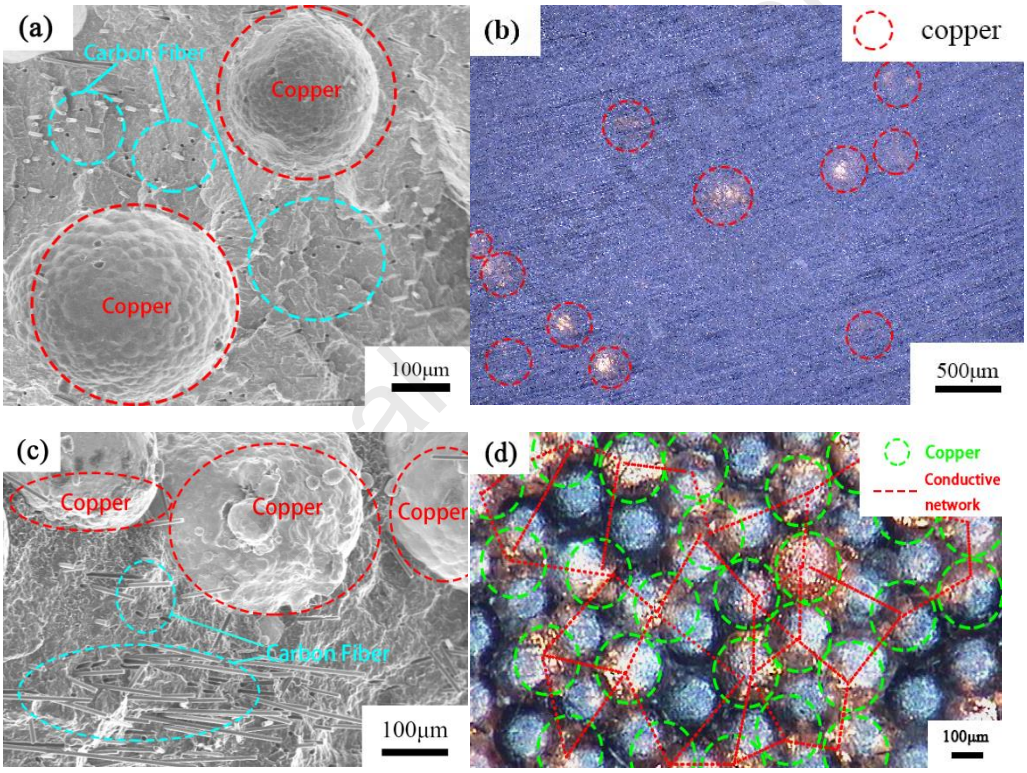

Figure 12. Morphology from (a) cross-sectional SEM and (b) optical photograph of PP composites prepared by a traditional hot embossing method and, (c) cross-sectional SEM and (d) optical microscopy photograph of the composites prepared by the anchoring array assembly method.

Figure 12 (a) shows that the CPs were located and arranged on one side of the sample, the CFs attached to CPs and PP and the distance between CPs was large at CP content 2 vol.%, and a conductive network was not formed. The CPs in the sample

prepared by the traditional hot embossing method were relatively well dispersed in the PP, while the anchoring array assembly method limited the positioning of the CPs, resulting in the CPs being arranged densely on one side, as shown in Figure 12 (c) and (d). The CPs overlap and form a conducting path. The CFs are constrained and form an "island-bridge" conductive network with dense contact points, thus resulting in a fourfold increase in electrical conductivity when the volume ratio of CF was ≥ 4 vol.%, as shown in Table 4.

A representative stress-strain curve for a composite prepared by both the traditional hot embossing and the anchoring array assembly methods is shown in Figure 13, i.e. with CF and CP content of 6 vol.% and 2 vol.%, respectively. The corresponding tensile test data is listed in Table 5.

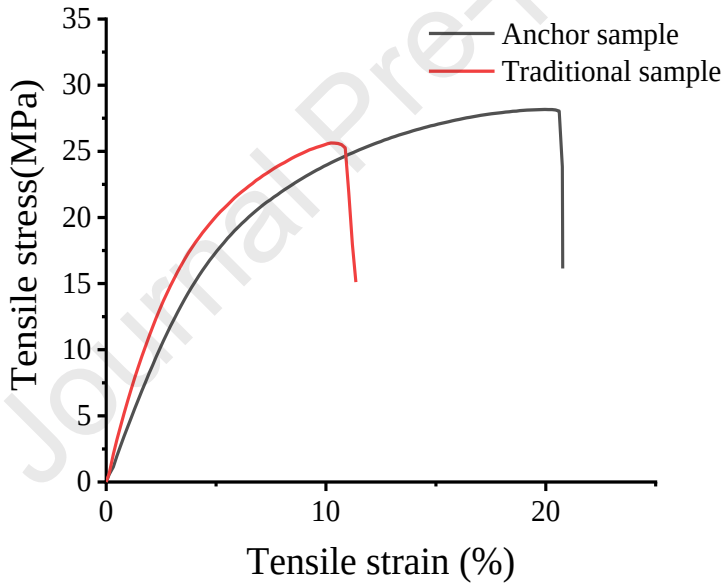

Figure 13. Representative stress-strain curves for a composite prepared by the traditional hot embossing and the anchoring array assembly methods

Table 5. Tensile test data comparing composite samples prepared by traditional hot embossing and anchoring array assembly methods, values in brackets are standard deviations.

Processing methods	Maximum tension value (N)	Maximum tensile stress (MPa)	Elastic Modulus (MPa)	Elongation at break (%)	Maximum energy of material (J)
Traditional hot embossing	632.36 (8.36)	25.29 (1.67)	503.57 (6.75)	9.65 (2.06)	0.41 (0.23)

Anchoring array assembly	704.13 (2.43)	28.17 (0.49)	390.26 (3.7)	20.00 (0.71)	1.08 (0.03)

From the tensile fracture test of the composite, it can be seen that compared with the traditional hot embossing processing method, for the anchoring array assembly method, the fracture stress and elongation at break of the PP/CP/CF composites are increased by 11.5 % and 107 %, respectively.

4. Conclusions

In this work, ternary conductive PP based composites were assembled by array anchoring and embossing. The strategy for using the array anchoring array assembly method was to use the array mold to confine the filler particles to a specific shape. When the PP matrix was extruded, the filler particles could not migrate, thereby increasing the filler density of the composites. It was found that when the inclination angle between the groove of the anchoring mold and the horizontal plane was greater than 11.5 °, the migration of CPs in the anchoring mold with the molten PP during hot embossing could be restricted. It was also found that the composites were most conductive when the CPs were densely arranged in a triangle. The conductivity of ternary composites of PP, CF and CP was measured on samples prepared by two methods: array anchor embossing and traditional hot embossing. Through the array anchoring embossing process, the densely arranged triangles of CP and CF formed a dense "island-bridge" conductive network in the PP matrix, where CPs acts as the "islands" and CFs as a "bridge". In the vertical direction, the mobility of CF and CP microspheres is limited, and both are anchored to each other, so that the two fillers are closely packed and overlapped in the horizontal plane, thereby further improving the conductivity of the composites. For the CP triangle network model, each CP is connected to six CPs, which increased the contact area between CPs, and improved the conductivity of composites made by the anchoring method by up to 52 times compared with the composites prepared with the traditional hot embossing method (i.e. for a CF content of 18 vol.% and CP content of 2 vol.%). Among all the samples prepared, the composites prepared by the anchoring array assembly method (thickness 0.2 mm, CF content 18 vol.% and CP content 2 vol.%) had the highest conductivity at

137.7 S/m. By comparing this work with that of others (as shown in Table S1), it was found that the conductivity of the composites described in this paper are higher and the method of preparation simpler to most other related methods. Compared with the traditional hot embossing method, the array anchor assembly method can easily arrange the CPs and CFs to form a regular triangular dense "island-bridge" conductive network in the PP matrix and improve the conductivity of the composite. It can be seen from the tensile fracture test results that, compared with the traditional hot embossing method, the fracture stress and elongation at break of the PP/CP/CF composites prepared using the anchoring array assembly method was increased by 11.5 % and 107 %, respectively.

5. Acknowledgements

This work was supported by National Nature Science Foundation of China (Grant No.52003018&52003019)

6. References

[1] Ma Y, Wu D, Liu Y, Li X, Qiao H, Yu ZZ. Electrically conductive and super-tough polypropylene/carbon nanotube nanocomposites prepared by melt compounding. Composites: Part B. 2014;56:384-91.

[2] Díez-Pascual AM, Naffakh M, Marco C, Gómez-Fatou MA, Ellis GJ. Multiscale fifiber-reinforced thermoplastic composites incorporating carbon nanotubes: a review. Current Opinion in Solid State & Materials ence. 2014;18:62-80.

[3] Sharma M, Gao S, Mäder E, Sharma H, Wei LY, Bijwe J. Carbon fiber surfaces and composite interphases. Composites ence & Technology. 2014; 102:35-50.

[4] Chung DDL. Comparison of submicron-diameter carbon filaments and conventional carbon fibers as fillers in composite materials. Carbon. 2001;39:1119-25.

[5] Ge Y, Xiang N, Wang B, Wang T, Yan Y. Effect of heat treatment after injection molding on the properties of polycarbonate. Polymer Materials Science and Engineering. 2019; 35:89-94.

[6] Ge Y, Wang T, Lang J, Li L, Yan Y. Effect of injection molding plasticizing process on the properties of polycarbonate. Polymer Materials Science and Engineering. 2017; 33:113-118.

[7] Xu YT, Wang Y, Zhou GG, Sun WJ, Dai K, Hua J, Lei T, Yan DX, Li ZM. An electrically conductive polymer composite with a co-continuous segregated structure for enhanced mechanical performance. Journal of Materials Chemistry C. 2020; 8:11546-11554.

[8] Cao Q, Song Y, Tan Y, Zheng Q. Conductive and viscoelastic behaviors of carbon black filled polystyrene during annealing. Carbon. 2010; 48:4268-4275.

[9] Deng H, Tetyana S, Emiliano B, Zhang R, Dirk L, Luca M, Fu Q, Ingo A, Ton P. Preparation of High-Performance Conductive Polymer Fibers through Morphological Control of Networks Formed by Nanofillers. Advanced Functional Materials. 2010; 20:1424-1432.

[10] Zhang QY, Wang JX, Zhang BY, Guo BH, Yu J, Guo ZX. Improved electrical conductivity of polymer/carbon black composites by simultaneous dispersion and interaction-induced network assembly. Composites Science and Technology. 2019;176:106-114.

[11] Cai J, Li XH, Ma L, Jiang YG, Zhang DY. Facile large-scale alignment and assembly of conductive micro/nano particles by combining both flow shear and electrostatic interaction. Composites Science and Technology. 2019;171:199-205.

[12] Christoph U, Tina M, Francesco P, Jiri D, David S, Claudia P, Christian F. Impact of fiber length and fiber content on the mechanical properties and electrical conductivity of short carbon fiber reinforced polypropylene composites. Composites Science and Technology. 2020;188:107998.

[13] Wu D, Gao X, Sun J, Wu D, Liu Y, Kormakov S, Zhen X, Wu L, Huang Y, Guo Z. Spatial Confining Forced Network Assembly for preparation of high-performance conductive polymeric composites. Composites: Part A. 2017; 102:88-95.

[14] Deng H, Lin L, Ji M, Zhang S, Yang M, Fu Q. Progress on the morphological control of conductive network in conductive polymer composites and the use as electroactive multifunctional materials. Progress in Polymer ence. 2014; 39:627-655.

[15] Jalalvanda AR, Roushani M, Goicoechea HC, Rutledge DN, Gu HW. MATLAB in electrochemistry：A review. Talanta. 2019; 194:205-225.

[16] Corbin MJ, Butler GF. Multisim：An object-based distributed framework for mission simulation. Simulation Practice and Theory. 1996; 3:383-399.

[17] Nan CW, Shen Y, Ma J. Physical Properties of Composites Near Percolation. Annual Review of Material Research. 2010; 40(1): 131-151.

[18] Sheng P. Fluctuation-induced tunneling conduction in disordered materials. Physical Review B. 1980; 21:2180.

[19] Simmons JG. Generalized Formula for the Electric Tunnel Effect between Similar Electrodes Separated by a Thin Insulating Film. Journal of Applied Physics. 1963; 34:1793.

[20] Simmons JG. Low-Voltage Current-Voltage Relationship of Tunnel Junction. Journal of Applied Physics. 1963; 34:238. doi: 10.1063/1.1729081.

[21] Simmons JG, Unterkofler GJ. Potential Barrier Shape Determination in Tunnel Junction. Journal of Applied Physics. 1963; 34:1828.

[22] Mohd R, Nabilah A, Sulong AG, Sahari J. A review of electrical conductivity models for conductive polymer composite. Journal of Hydrogen Energy. 2016; 42:9262-9273.

[23] Taipalus R, Harmia T, Zhang MQ, K Friedrich. The electrical conductivity of carbon-fibre-reinforced polypropylene/polyaniline complex-blends: experimental characterisation and modelling. 2001; 61(6):801-814.

[24] Wu ZL, Wang SX, Zhang LH, Hu S.Jack. An analytical model and parametric study of electrical contact resistance in proton exchange membrane fuel cells. Journal of Power Sources. 2009; 189:1066-1073.

[25] Holm R. Electric Contacts Theory and Application. Springer-Verlag. New York. 1967: 9-23.

[26] Greenwood JA. Constriction resistance and the real area of contact. British Journal of Applied Physics. 1966; 17(12): 1621-1632.

[27] Ashutosh R, Bhargava S, Kumar V. Testing the Validity of Greenwood and Tripp's Sum Surface Assumption for Elastic-Plastic Contact. Journal of Tribology. 2020; 142: 101501.

[28] Johnson KL. Normal contact of elastic solids-Hertz theory. Contact Mechanics. 1985, 84-106. doi:10.1017/cbo9781139171731.005.

[29] Weber M, Kamal MR. Estimation of the volume resistivity of electrically conductive composites. Polymer Composites. 1997, 18(6): 711–725.

[30] Guan Q, Cheng JL, Li XD, Wang B, Huang L, Nie FD, Ni W. Low Temperature Vacuum Synthesis of Triangular CoO Nanocrystal/Graphene Nanosheets Composites with Enhanced Lithium Storage Capacity. Scientific Reports. 2015, 5: 10017.

[31] Xu SG, Berdyugin AI, Kumaravadivel P, Guinea F, Kumar RK, Bandurin DA, Morozov SV, Kuang W, Tsim B, Liu S, Edgar JH, Grigorieva IV, Fal'ko VI, KimM, Geim AK. Giant oscillations in a triangular network of onedimensional states in marginally twisted graphene. Nature Communication. 2019, 10: 4008.

[32] Zhang H, Zhang X, Li D, Yang X, Wu D, Sun J. Thermal conductivity enhancement via conductive network conversion from "sand-like" to "stone-like" in the polydimethylsiloxane composites. Composites Communications. 2020; 22: 100509.

[33] Ibrahim K, Sukru K, Fahrettin Y. Electrical characterization of graphene oxide and organic dielectric layers based on thin film transistor. Applied Surface Science. 2014; 318:74-78.

[34] He X, Huang Y, Wan C, Zhao X, Kormakov S, Gao X, Sun J, Zheng X, Wu D. Enhancing thermal conductivity of polydimethylsiloxane composites through spatially confined network of hybrid fillers. Composites Science and Technology. 2019; 172:163-171.

[35] Iijima S. Helical microtubules of graphitic carbon. Nature. 1991; 354:56-58.

[36] Nabilah AMR, Abu BS, Jaafar S. A review of electrical conductivity models for conductive polymer composite. 2017; 42:9262-9273.

[37] Corinna G, Mohamad AR, Aapo V, Kestutis G, Daniel M, Bernhard W, Pierre OC, Severine G, Mika P. Microfabricated sensor platform with through-glass vias for

bidirectional 3-omega thermal characterization of solid and liquid samples. Sensors and Actuators A： Physical. 2018; 278:33-42.

[38] Leire S, Martin VD, Ruth C, Antxon S, Gerrit WMP, Alejandro JM. Effect of shear rate and pressure on the crystallization of PP nanocomposites and PP/PET polymer blend nanocomposites. Polymer. 2020; 186:121950.

Conflict of interest statement

We declare that we have no financial and personal relationships with other people or organizations that can inappropriately influence our work, there is no professional or other personal interest of any nature or kind in any product, service and/or company that could be construed as influencing the position presented in the manuscript entitled “An Anchoring Array Assembly Method for Enhancing the Electrical Conductivity of Composites of Polypropylene and Hybrid Fillers”.

Declaration of interests

☒ The authors declare that they have no known competing financial interests or personal relationships that could have appeared to influence the work reported in this paper.

☐The authors declare the following financial interests/personal relationships which may be considered as potential competing interests: